

Formulation and Evaluation of P-Naphthoquinone Casein Nanodispersions and their Antibacterial and Anticancer Activities

Anitha Manikandan Duraikannu¹, Shanmugaprakash Muthusamy^{1,*}, Thangavel Pichaiapaa Rajesh²

¹Department of Biotechnology, Kumaraguru College of Technology, Coimbatore, Tamil Nadu, INDIA.

²Department of Biotechnology, UCE BIT Campus Anna University, Tiruchirapalli, Tamil Nadu, INDIA.

ABSTRACT

Aim/Background: This study focuses on the preparation, characterization, and evaluation of nanodispersion formulations of casein and PNQ for their antibacterial and anticancer activities. Casein micelles were used to stabilize PNQ precipitates, aiming to enhance bioavailability and therapeutic efficacy. **Materials and Methods:** Nanodispersion formulations were prepared and characterized using a Zeta sizer to determine particle size and stability. The average particle size ranged between 230 nm and 350 nm, with a Dynamic Light Scattering (DLS) potential of -17.6 mV to -17.2 mV, indicating stability due to casein-induced micelle formation. FTIR analysis confirmed the presence of casein-micelle-stabilized PNQ particles. *In vitro* drug release studies were conducted to assess the efficiency of the formulation. **Results:** The optimized formulation, S6, exhibited a zeta size of 229 nm, a stabilized zeta potential of -17.6 to -17.2, and a rapid drug release within 15 minutes, achieving a high drug content of 89.76±3.7%. Antimicrobial activity was observed against both *E. coli* and *S. aureus*. Cytotoxicity assay (MTT) revealed an IC₅₀ value of 46.35±0.05 µg for the drug nanodispersion, indicating potential anticancer properties. **Conclusion:** The prepared PNQ nano formulation (S6) demonstrated promising antibacterial and anticancer properties by improving bioavailability and drug release. These findings suggest its potential application in treating microbial infections and cancer.

Keywords: Antibacterial, Anticancer, Casein Nanodispersion, p-Naphthoquinone.

Correspondence:

Shanmugaprakash Muthusamy

Department of Biotechnology,
Kumaraguru College of Technology,
Coimbatore-641035, Tamil Nadu, INDIA.
Email: shanmugaprakash.m.bt@kct.ac.in

Received: 11-04-2025;

Revised: 28-05-2025;

Accepted: 07-09-2025.

INTRODUCTION

Nanotechnology facilitates the administration of medications with low water solubility and offers a method of circumventing the liver, therefore avoiding first metabolism. Nanotechnology enhances the bioavailability of orally administered medications by its distinctive absorption processes, such as absorptive endocytosis. Furthermore, it has the ability to remain in its circulatory system for an extended duration, gradually releasing the medication in a regulated manner, hence minimizing variations in plasma levels and adverse reactions. Nanotechnology has the potential to enable the production of materials that are lighter, stronger, and programmable, while also requiring less energy compared to traditional materials.¹ The research findings indicate that Engineered Nanoparticles (ENPs) can have both beneficial and detrimental impacts on the growth and maturation of plants. The effect of ENPs on plants is influenced by factors such as the

constitution, quantity, shape, and physicochemical properties of the ENPs, as well as the specific plant species.² Researchers have proven and widely employed further nanoparticles as potential drug carriers for cancer treatment, and their role in preventing drug resistance is impeccable.^{3,4}

In recent times, there has been a growing appreciation for nanomedicines due to their potential as delivery agents. These nanostructures can encapsulate or attach therapeutic drugs, enabling more precise delivery to target tissues with controlled release. Polymers that diffuse with organic solvents deform at the interface and incorporate bioactive compounds. Emulsifiers present in the aqueous phase serve as stabilizers the nanoparticles and hinder their tendency to aggregate. Next, the organic phase was removed from the nanodispersion using low pressure evaporation. The solvent-displacement technique is limited to water-miscible solvents that are organic and requires careful selection of the appropriate organic solvent. However, it allows for the creation of nanodispersions in one step having minimal use of energy and higher encapsulation efficiency.^{5,6}

Naphthoquinones are phytoconstituents that occur as secondary metabolites in plants and microorganisms; they have a substantial



DOI: 10.5530/ijper.20261335

Copyright Information :

Copyright Author (s) 2026 Distributed under
Creative Commons CC-BY 4.0

Publishing Partner : Manuscript Technomedia. [www.msttechnomedia.com]

impact on biooxidative processes and chemical defense. Traditional Indian medicine distinguishes naphthoquinones that are naturally occurring from plants such as lapachol, lawsone, juglone, and plumbagin.⁷ The pharmaceutical and agrochemical industries widely use Para-Naphthoquinone (PNQ), also known as 1,4-naphthoquinone, as a raw material. PNQ has garnered significant attention in biomedical research due to its remarkable pharmacological properties. Initially recognized for its potent anti-malarial effects, PNQ has emerged as a promising candidate for therapeutic interventions beyond malaria treatment. Recent studies have unveiled their intriguing potential in combating tumors, highlighting its multifaceted role in oncological research.^{8,9} A number of studies have demonstrated the synthesis, physico-chemical evaluation, and anticancer activity of PNQ and its derivatives.^{10,11} Prachayasittikul *et al.*, conducted a study where they synthesized derivatives of PNQ, did QSAR investigations, and evaluated their activity against cancer.¹² Experiments assessed the cytotoxicity of amino naphthoquinones against cancer cells of humans *in vitro*.¹³ This study was conducted within the context of a preliminary assessment process to determine these samples' potential antitumor properties. The strains of human carcinoma cells that were used were glioblastoma-human (SF-295), Melanoma (MDAMB-435), Colon Carcinoma (HCT-8 and 116), Leukemia (HL-60), Ovarian Carcinoma (OVCAR-8), human broncho-alveolar lung cancer, and prostate carcinoma (PC3-M). The National Cancer Institute, USA, which tests over 10,000 samples annually, uses the MTT method for cytotoxicity analysis. The MTT method of cytotoxicity research makes it simple to define cytotoxicity, but not its mechanism of action (Kumar, Mallya, Jain, 2020). The theranostic conjugates of curcumin-PNQ loaded onto mesoporous silica nanoparticles exhibited potent anticancer effects.¹⁴

Pharmaceutical products widely use proteins as nano-carrier systems due to their minimal cytotoxicity, biocompatibility and biodegradability, abundant sourcing from renewable sources, strong ability to connect to other molecules, effective targeting of specific body sites, and efficient cell uptake.¹⁵ Casein, a type of milk protein, provides all the amino acids to the body, which helps build muscle. When compared to other proteins, casein protein is digested more slowly, thus reducing the appetite and enhancing the feeling of fullness. The casein constituents, α_1 -, α_2 -, β -, and κ -casein, are in the ratios of 4:1:4:1 w/w, respectively, with an average pH of 4.8. Casein can be generally described as a block copolymer of hydrophobic and hydrophilic amino acid residues, and hence casein easily transforms into spherical micelles.^{16,17} Casein has demonstrated its potential as a carrier for biologically active agents.¹⁸ To the best of our knowledge literature on nanodispersion formulation of PNQ using casein as carrier was not found. Hence, in this study, nanodispersions were prepared and characterized and evaluated nanodispersion formulations of casein and PNQ for their antibacterial and anticancer activities.

MATERIALS AND METHODS

Chemicals

Potassium dihydrogen phosphate (KH_2PO_4 , 99%), lactic acid ($\text{CH}_3\text{CH}(\text{OH})\text{COOH}$, 88-92%), sodium hydroxide pellets (NaOH , >98%), ethanol ($\text{C}_2\text{H}_5\text{OH}$, >95%), methanol (CH_3OH , 99.8%), calcium chloride (CaCl_2 , 99%), and para-naphthoquinone ($\text{C}_{10}\text{H}_6\text{O}_2$, $\geq 97\%$) were purchased from Merck Limited, Mumbai, India. Pasteurized cow milk was purchased from the local market. Distilled water was prepared using a quartz double distillation unit (3365, Borosil Limited, Mumbai, India). DMEM/F12, Fetal Bovine Serum (FBS), Pen Strep, and Trypsin procured from Invitrogen Pvt. Ltd., Bangalore, India. Hep-G2 cells obtained from ATCC (HiMedia Laboratories Pvt. Ltd., Thane, India).

Preparation of casein polymer

Fifty millilitres of cow milk was centrifuged for 20 min at 5000 rpm at 4°C (Remi CM-12 Plus) to prepare casein. The upper layer of fat was removed. Three milliliters of calcium chloride (75 mM) solution was added to the remaining milk and adjusted the pH to 5 using lactic acid (1 M). After adjusting the pH and centrifuging the constituents for 10 min at 5000 rpm, The separated casein polymer precipitate was collected and used it for the nanodispersion formulation.¹⁹

Determination of λ_{max} of PNQ

PNQ (0.01 mg) was dispersed in 2 mL of methanol and sonicated it for 15 min using an ultrasonic bath sonicator (LJ-321, Lab Junction, Panchakula, India). A UV-visible spectrophotometer was then used (Lambda 35, Perkin Elmer, USA) to scan the solution for wavelengths at which the strongest photon absorption (λ_{max}) observed in the wavelength range between 300 and 700 nm at a resolution of 1 nm.

Construction of Calibration curve of PNQ

A 2 mg sample of PNQ was evenly distributed in 2 mL of methanol and subjected it to 15 min of sonication using an ultrasonic bath sonicator (LJ-321, Lab Junction, Panchakula, India). One milliliter was extracted from the previous solution and diluted it with pH 7.4 phosphate buffer to a final volume of 10 mL, creating a stock solution. Volumes of 0.5, 1, 1.5, 2, and 2.5 mL were dilute to final volumes of 10 mL each using a pH 7.4 phosphate buffer to create serial dilutions. The PNQ concentrations of 0.5, 1, 1.5, 2, and 2.5 $\mu\text{g}/\text{mL}$ were estimated using a UV-visible spectrophotometer against a blank pH 7.4 phosphate buffer, based on the PNQ maximum as previously determined.

Preparation of nanodispersions

PNQ nanodispersions were prepared using two levels of casein (200 and 400 mg), stirring rates (700 and 1400 rpm), and homogenization times (15 and 30 min). Typically, 200 mg of casein was dissolved in 20 mL of a 10 mM calcium chloride

solution and stirred continuously for 1 h. Next, 100 mg of PNQ was dissolved in 2 mL of methanol and sonicated it for 15 min. This PNQ solution was added to the above casein solution and the above two solutions were then continuously stirred for 24 h to encapsulate PNQ in a case in nanodispersion. The nanodispersions were assessed using various techniques as detailed in the following sections.^{20,21}

Particle size analysis

The formation of PNQ and casein nanodispersion was analyzed and measured their average size using particle size analysis. 1 mL of the formulation was taken and diluted it to 20 mL using distilled water. Then, 2.5 mL of the formulation was taken in a disposable cell with four openings and used a Dynamic Light Scattering (DLS) analyzer (NanoPlus, Micromeritics Instrument Corp., USA) at 25°C to measure the average particle size.

Zeta-potential measurement

DLS was used to measure the particle charge and determine whether the colloid or dispersion was stable. The charge of the particle determined the stability of the colloid. An Electrophoretic Light Scattering (ELS) analyzer (NanoPlus, Micromeritics Instrument Corp., USA) was used to find out the zeta-potential the formulated nanodispersions. This analyzer finds the electrophoretic mobility of particles from 3 nm to 10 μm in a range of sizes using the laser doppler velocity technique. The temperature was set at 25 °C during the measurement and the pH of the nanodispersions was at 7.²²

Scanning Electron Microscopy (SEM)

The SEM employs an electron beam with high energy systematically examining the surface of the sample using a raster image pattern. Electrons engage in interactions with the atoms comprising the sample, generating signals that encompass details regarding the sample's surface topography, composition, and additional attributes, such as electrical conductivity. The morphological features of PNQ nanodispersion powder were examined using SEM. The experiment was conducted using a scanning electron microscope (EVO 18, Carl Zeiss, Germany). Before testing, the samples were affixed to an aluminum stub using double-sided adhesive tape and rendered them electrically conductive by applying a thin 200 nm thickness gold layer in a vacuum. A scanning electron microscope with an acceleration voltage was used of 0.5 kV and a resolution of 4000.²³

FT-IR analysis

FT-IR Spectrometer (Spectrum Two, Perkin Elmer, USA) with LiTaO₃ Detector and KBr window. One drop of the liquid sample was placed on the crystal window and performed scanning. One milligram of pure KBr was mixed with 0.2 mg of the solid sample in a 10:2 ratio, placed it into the sample holder, and then

performed the scanning. Data were collected over a spectral range between 4000 and 400 cm⁻¹ at a resolution of 0.5 cm⁻¹.²⁴

X-ray diffraction (XRD) analysis

XRD is a method employed to ascertain the atomic arrangement within crystalline substances. It can also reveal the arrangement of atoms in non-crystalline materials, referred to as the short-range order. These data enable the determination of the lattice constants and phases mean size of grain, degrees of crystallinity, and structural defects of crystals. Advanced XRD techniques yield precise data on strain, roughness, crystal symmetry, and density of electrons. When radiation hits a solid, it is coherently scattered by atoms that are spaced out at regular intervals. This creates beams that are spread out in different directions. Samples of single-crystals produce spot patterns, while Samples composed of several crystalline structures produce ring patterns. The identification of a specific crystal structure can be accomplished by analyzing the pattern, intensity, and location of the diffraction peaks, which are characterized by the Bragg angle, θ or interplanar spacing d_{hkl} .

$$D = \frac{k\lambda}{\beta \cos \theta}$$

where D is average crystal size, K is Scherrer constant (0.94), λ is wavelength of X-ray (1.5406 Å), β is broadening of lines at half of the maximum intensity (radians), θ is half of the Bragg's angle.²⁵

Determination of drug content

To determine the drug concentration, a 0.2 mL sample was extracted from the above formulations and mixed with 500 μL of methanol. After sonicating the mixture for 15 min, the resulting solution was diluted to a final volume of 2 mL using methanol. A volume of 0.2 mL was taken from this solution and diluted it to a total volume of 2 mL using a pH 7.4 buffer. A UV-visible spectrophotometer (Lambda 35, Perkin Elmer, USA) was employed to measure the optical density of the solution at the maximum wavelength (λ_{max}) of 339 nm. This was done with a pH 7.4 buffer solution as a blank solution. The drug content (%) was determined for all eight formulations in triplicate.

In vitro drug release

A simulation was conducted to study the release of the drug in the human body using a semipermeable dialysis membrane tube made of cellulose with a molecular weight ranging between 12,000 and 14,000 (dialysis membrane 50, LA387, HiMedia Laboratories Pvt. Ltd., India). The pH of the solution was regulated to 7.4 using phosphate buffer to replicate the pH of blood. In vitro PNQ release tests were conducted in triplicate using eight formulations. Typically, 200 μL of the formulation and 800 μL of pH 7.4 buffer were introduced into the dialysis membrane tube. The tube was immersed in a beaker consisting of 100 mL of pH 7.4 buffer dissolution medium, maintaining a constant speed of 200 rpm. Then, 1 mL aliquots of the samples

were withdrawn from the dissolution medium at intervals of 0.25, 0.5, 1, 2, 3, 5, 6, 7, and 8 hr. Following the withdrawal of 1 mL of the dissolving liquid, The withdrawn volume was replenished with 1 mL of pH 7.4 buffer. The drug concentration in the medium was quantified using a UV-visible spectrophotometer using pH 7.4 buffer as the reference solution.^{26,27}

Antimicrobial assay

The antibacterial efficacy of the PNQ nanodispersion samples was assessed by employing the well diffusion technique on nutrient agar. The control (chloramphenicol) and test samples (PNQ and PNQ nanodispersion) were prepared for anti-bacterial studies by dissolving 10 mg/mL in distilled water. Two bacterial strains, *S. aureus* (ATCC 25923) and *E. coli* (ATCC 10536), were used as benchmarks for antibacterial analysis. The bacterial strains were introduced into nutrient agar plates using aseptic techniques. A glass L-rod was used to spread the culture, applying 100 μ L of the developed culture. Then, a round punching cork was used to make five 8-mm wells on each plate. The control was put in the middle, and the test samples (PNQ and nanodispersion of PNQ at concentrations of 25, 50, 75, and 100 μ L) were put in the four other wells. The plates were then heated to 37°C and left there for 24 h. Once the incubation period concluded, the zone of inhibition was measured and reported. The Minimum Inhibitory Concentration (MIC) is the lowest concentration at which the growth of the particular microbial species is fully inhibited. The experiments were conducted three times to ensure accuracy and reliability.^{28,29}

Cytotoxicity analysis by MTT assay

Hep-G2 cell cultures were obtained from ATCC A cytotoxicity assay was conducted using the MTT method at the BioMe Live, Karaikudi, Tamil Nadu, India. Humidified air was maintained at a temperature of 37 °C with 5% CO₂. Stock cells were cultivated in DMEM/F12 medium supplemented with 10% deactivated fetal bovine serum, penicillin (100 IU/mL), and streptomycin (100 μ g/mL). To separate the cells, a cell dissociating solution was employed consisting of trypsin (0.2%), EDTA (0.2%), and glucose (0.05%) in PBS. The viability of the cells is assessed after undergoing centrifugation. In addition, 50,000 Jurkat cells were introduced into each well of a 96-well plate and allowed the plate to incubate for 24 hr at a temperature of 37°C with a CO₂ concentration of 5%. The monolayer cell culture was enzymatically dissociated using trypsin and then standardized the cell concentration to 1.0x10⁵ cells/mL using the appropriate media supplemented with 10% Fetal Bovine Serum (FBS). A 100 μ L of the diluted cell solution containing 50,000 cells per well was added to 96-well microtiter plate. A partial monolayer was established within 24 hr. The liquid portion was discarded, the single layer of cells was rinsed once with a solution, and 100 μ L of various concentrations of the test drug were introduced to the

incomplete layer of cells in microtiter plates. Subsequently, the plates were placed in an incubator set at a temperature of 37 °C for a duration of 24 hr, while maintaining a 5% concentration of CO₂ in the environment. After the incubation period, the test solutions in the wells were taken out, and 100 μ L of MTT solution (5 mg/10 mL of MTT in PBS) was introduced into each well. The plates were placed in an incubator for duration of 4 hr at a temperature of 37°C, within an environment containing 5% CO₂. The liquid above the sediment was extracted, and 100 μ L of Dimethyl Sulfoxide (DMSO) was introduced. The plates were then gently agitated to dissolve the formazan that had been produced. The absorbance was quantified by using a microplate reader at a specific wavelength of 590 nm. The following formula was employed to calculate the growth inhibition (%) and produced the dose-response plots for each cell line to ascertain the concentration of the test agent required to impede cell growth by 50% (IC₅₀). The inhibition (%) was determined by applying the given formula.^{30,31}

$$\% \text{ Inhibition} = 100 - \left(\frac{\text{Optical density of sample}}{\text{Optical density of control}} \right) \times 100$$

IC₅₀ Calculation

IC₅₀, or half of the maximum inhibitory concentration, quantifies the potency of a substance in suppressing biological or metabolic activity. This measure quantifies the amount of an inhibitor chemical or substance required to decrease the inhibition of a biological process (or one of its components, such as an enzyme, cell, receptor, or microbe) by 50%.^{32,33}

To calculate the IC₅₀ of a drug, one can design a dose-response plot and analyze the impact of various antagonist doses to reverse agonist action. The IC₅₀ values for a specific antagonist can be determined by ascertaining the concentration required to inhibit 50% of the maximal biological reaction generated by the agonist. The IC₅₀ values for cytotoxicity testing were obtained by a nonlinear regression analysis, specifically a curve fit, following a sigmoid dose response curve. These values were calculated using Prism 6 (Graph Pad, San Diego, CA, USA).

RESULTS AND DISCUSSION

Calibration curve of PNQ

The PNQ solution was scanned to determine the maximum absorbance (λ_{max}) in the UV region. A peak at a wavelength of 339 nm was observed in Figure 1, which illustrates the wavelength vs. absorbance of PNQ. Figure 2 displays a typical plot of PNQ concentration against absorbance. The curve exhibited linearity in the concentration range between 0.5 and 2.5 μ g/mL for PNQ, as measured at a wavelength of 339 nm. The regression equation of the calibration curve was determined as $y = 0.1512x + 0.0144$, and found a regression coefficient (R²) of 0.9967, indicating the curve's linearity.

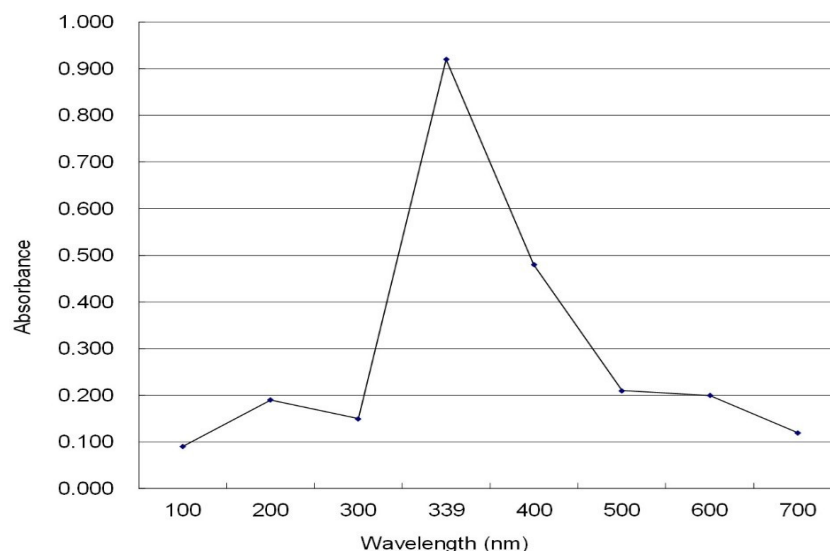


Figure 1: Determination of absorption maximum of PNQ.

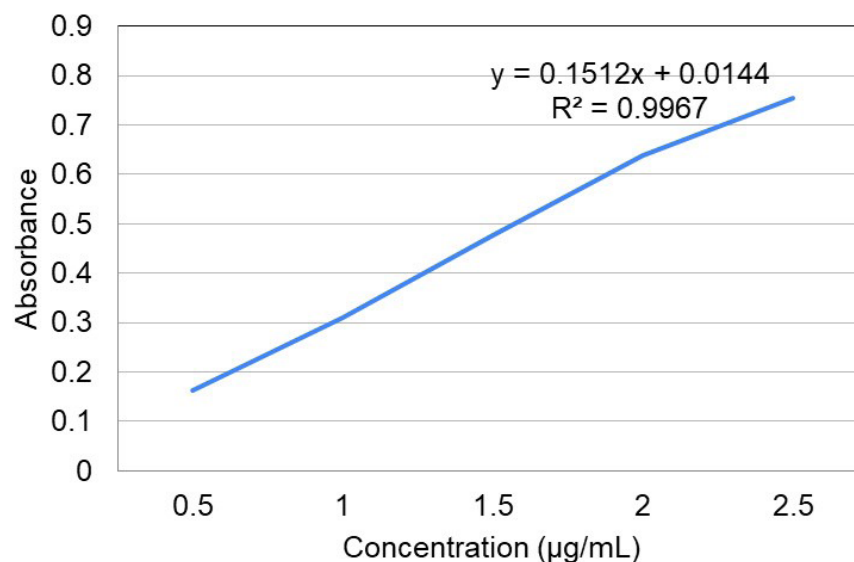


Figure 2: Calibration curve of PNQ.

Particle size analysis

The Dynamic Light Scattering (DLS) method was employed to measure the particle's charge and determine the stability of the colloid or dispersion. The Zeta sizer was used to measure the particle size of the casein and PNQ nanodispersion. The particle size of formulation S6 was found to be 229 nm (Figure 3A). The Polydispersity Index (PI) was found to be 0.240 indicating that the maximum number of particles were uniform in size.

Zeta-potential evaluation

The zeta potential of the nanodispersions was measured employing the Zetasizer Electrophoretic Light Scattering (ELS) analyzer (NanoPlus, Micromeritics Instrument Corp., USA), which uses the laser doppler velocity method for quantifying the electrophoretic motion of the particles with a size range between

3 and 10 nm. The formulation dispersion (S6) was stable when the charge of the particle ranged between -25 mV and 25 mV. The result showed that the charge of the PNQ formulation S6 ranged from -17.6 mV -17.2 mV, indicating its stability, as illustrated in Figure 3B.

Scanning electron microscopy

The external morphology of pure PNQ and formulated nanoparticles was evaluated using SEM.³⁴ The representative photomicrographs in Figure 4A to 4D showed three distinct patterned shapes of surface morphology of pure PNQ: irregularly shaped particles with wrinkles, spherical particles, and spherical particles with wrinkles. Figure 4E to 4H showed that the shape of the nanoparticles was distinct from the pure PNQ, which confirmed the presence of PNQ inside the casein micelles.

Fourier transform infrared analysis

FT-IR spectroscopy is a method used to capture and analyze infrared spectra that are helpful in structure determination (Figure 5).^{35,36} The main peaks (3396 and 1648 cm^{-1}) observed were caused by OH stretching and deformation. The bands between 407 and 591 cm^{-1} were caused by the C-C-C chain bending vibration of the alkyl chain. The band between 1650 - 1600 cm^{-1} indicates C=C stretching, whereas the band at 3622 cm^{-1} assigned to the absorption peak that appeared around casein. Next, the peak that

appeared at around 3700 - 3584 cm^{-1} was due to the stretching vibration of O-H bond (Agarwala, Rohani, Hastings, 2022). The FTIR spectra confirmed the presence of PNQ and casein in formulation S6.

X-ray diffraction analysis

XRD analysis of materials, typically in powder materials. XRD analysis was used to determine the crystallite size. XRD has a wide variety of applications such as crystalline structure,

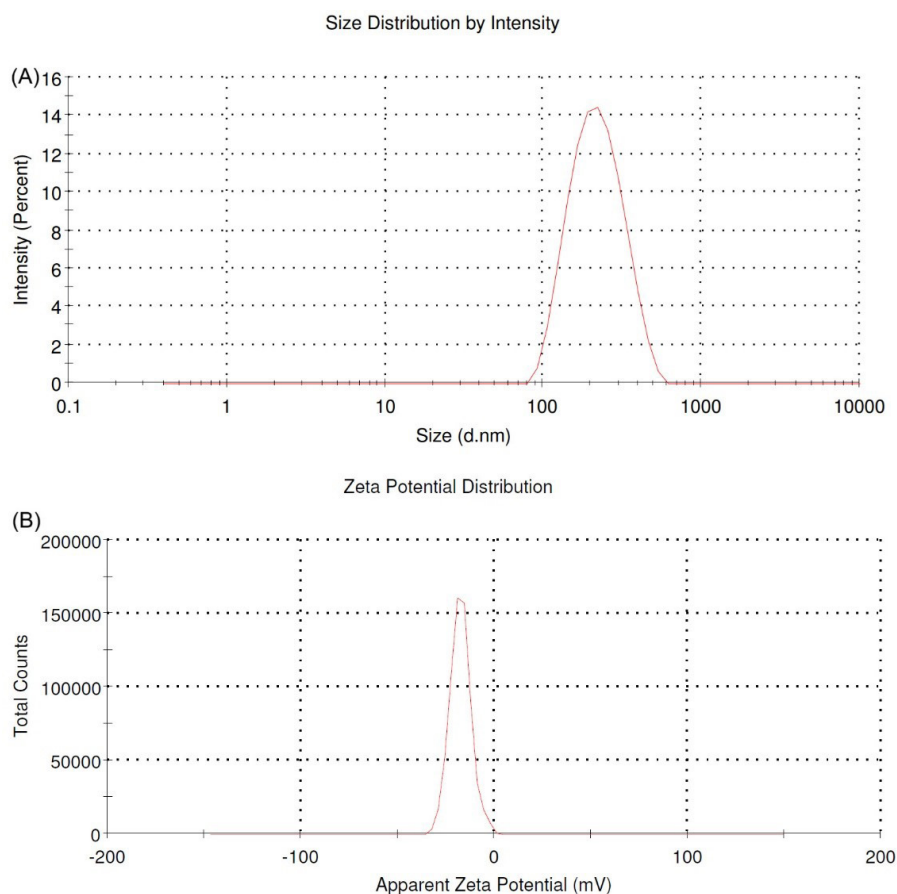


Figure 3: (A) Particle size analysis and (B) Zeta potential of PNQ formulation (S6).

Table 1: Total drug content and maximum drug released based on formulation parameters ($n=3$).

Formulation code	Formulation parameters			Drug content (%)	Maximum drug release	
	Casein (mg)	Stirring rate (rpm)	Homogenization time (min)		PNQ released (%)	Time (min)
S1	200	700	15	75.59±3.56	40.74±2.03	60
S2	200	1400	15	79.25±4.17	50±2.5	30
S3	400	700	15	51.48±3.72	18.25±0.9	30
S4	400	1400	15	59.12±2.84	22.22±1.11	30
S5	200	700	30	78.51±4.10	49.43±2.4	30
S6	200	1400	30	89.76±3.7	75.13±2.2	15
S7	400	700	30	66.11±2.28	29.49±1.4	30
S8	400	1400	30	76.77±3.82	46.03±2.3	30

The results are the Mean±SD of three experiments.

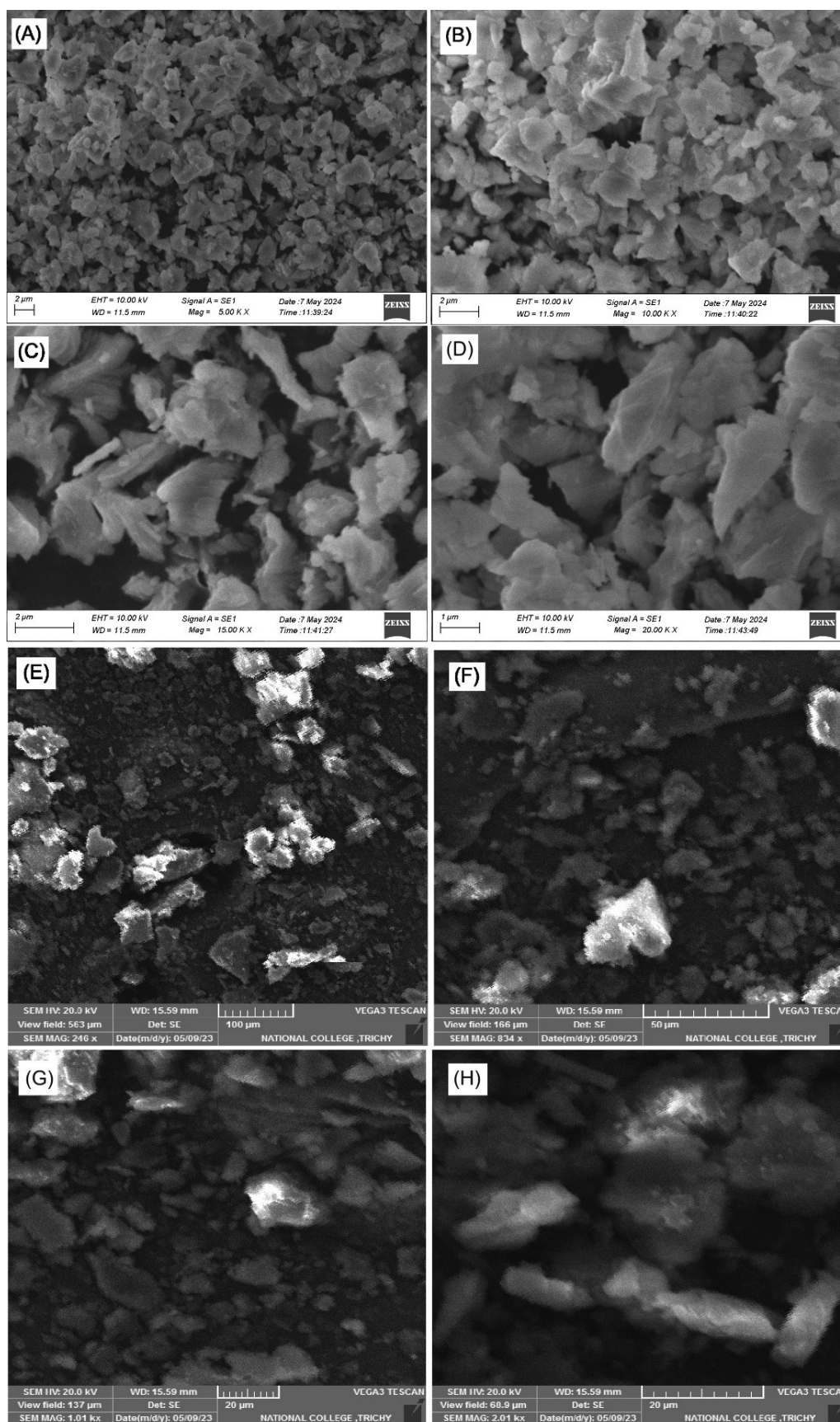
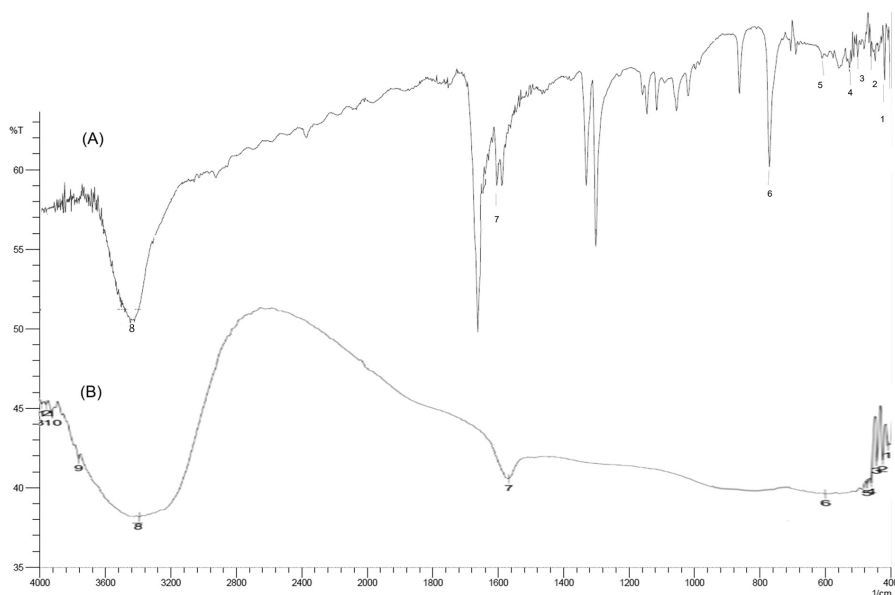


Figure 4: Micrographs of pure PNQ at magnifications: (A) 5 KX, (B) 10 KX, (C) 15 KX and (D) 20 KX, and PNQ nanodispersion at magnifications: (E) 246 X, (F) 834 X, (G) 1.01 KX and (H) 2.01 KX.

Table 2: Antimicrobial assay of pure PNQ and PNQ nano dispersion formulation (S6).

Strain	Zone of inhibition (mm)									
	Control	PNQ solution (µL)				Control	PNQ nanodispersion (µL)			
		25	50	75	100		25	50	75	100
<i>E. coli</i>	16	12	13	14	15	16	-	11	11	12
<i>S. aureus</i>	19	13	14	15	16	17	-	9	10	11

**Figure 5: FTIR spectra of (A) pure PNQ and (B) PNQ formulation (S6).**

chemical composition, orientation and phase identification Figure 6. The diffraction peaks were recorded in the 2θ range was 25 to 30° . From the graph, it can be interpreted that the casein-encapsulated PNQ nanoparticles in formulation S6 was found to be semicrystalline in shape. From the given formula, the D value (average crystal size) was calculated as 6.318 nm.^{37,38}

Drug content in formulation

Table 1 shows the total amount of drug in PNQ nanodispersion based on casein concentration, stirring rate, and homogenization time, among other formulation parameters. Maximum drug entrapment was observed in those formulations (S4, S7, and S8) that underwent higher casein concentrations, stirring rates, and homogenization times. However, with formulation parameters of casein (200 mg), stirring rate (1400 rpm), and homogenization time (30 min), formulation S6 demonstrated a drug content of $89.76 \pm 3.7\%$, suggesting that one can use less casein to achieve nearly similar drug entrapment.

In vitro drug release studies

The drug released through the semi-permeable membrane (i.e., the dialysis membrane) was measured using UV spectrometry. Table 1 shows that the formulated linearity of the PNQ drug allows for the determination of the drug's concentration. The

formulation S6 released $75.13 \pm 2.2\%$ within 15 min (Elzoghby, El-Fotoh, Elgindy, 2011).

For new dosage forms like nanoparticles that don't have any regulatory or standard guidelines, *in vitro* drug release assessment becomes more important as a way to show how well the product works and how well it meets quality standards. Various approaches have been employed, each with its own benefits and limitations in terms of setup simplicity, sampling, and quick buffer substitution. An ideal *in vitro* drug release technique should accurately replicate *in vivo* circumstances and release processes, allowing for the formation of an *in vitro-in vivo* correlation (IVIVC) (D'Souza, 2014).

Antimicrobial assay

Table 2 and Figure 7 display the results of antimicrobial studies. It took 16 and 17 mm for *E. coli* and *S. aureus* for the control drug (chloramphenicol) to reach the PNQ solution, which is closer to the zone of inhibition. PNQ and its nanodispersion formulation (S6) showed antimicrobial activity against both *E. coli* and *S. aureus*. However, the PNQ formulation (100 µL) had a smaller zone of inhibition (12 and 11 mm) compared to the PNQ solution (100 µL), which was 15 and 16 mm for *E. coli* and *S. aureus*. This means that the formulation released PNQ more slowly as compared to control.

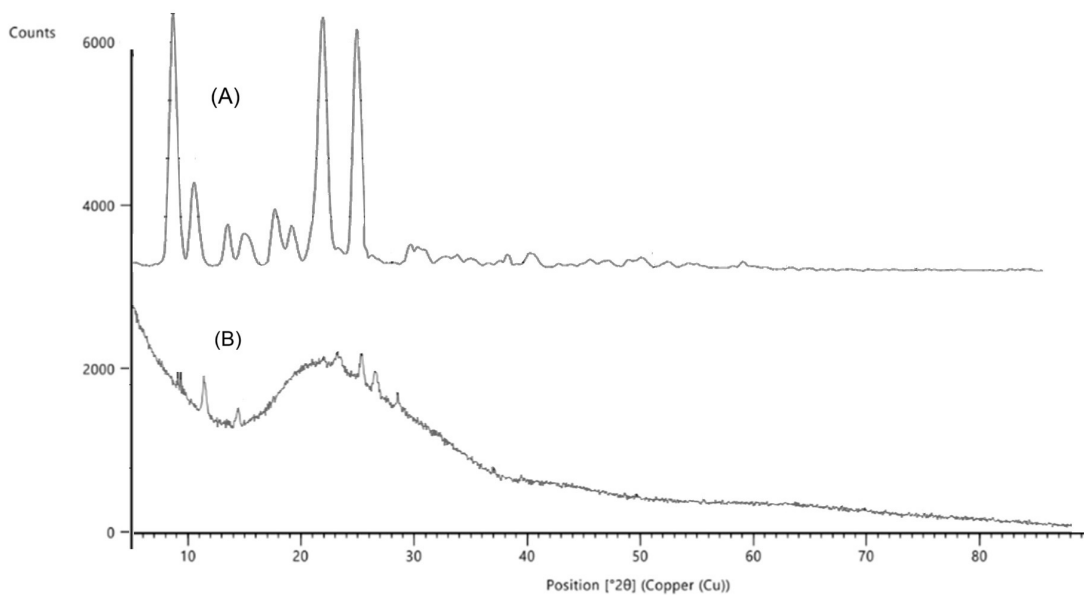


Figure 6: XRD spectra of (A) pure PNQ and (B) PNQ formulation (S6).

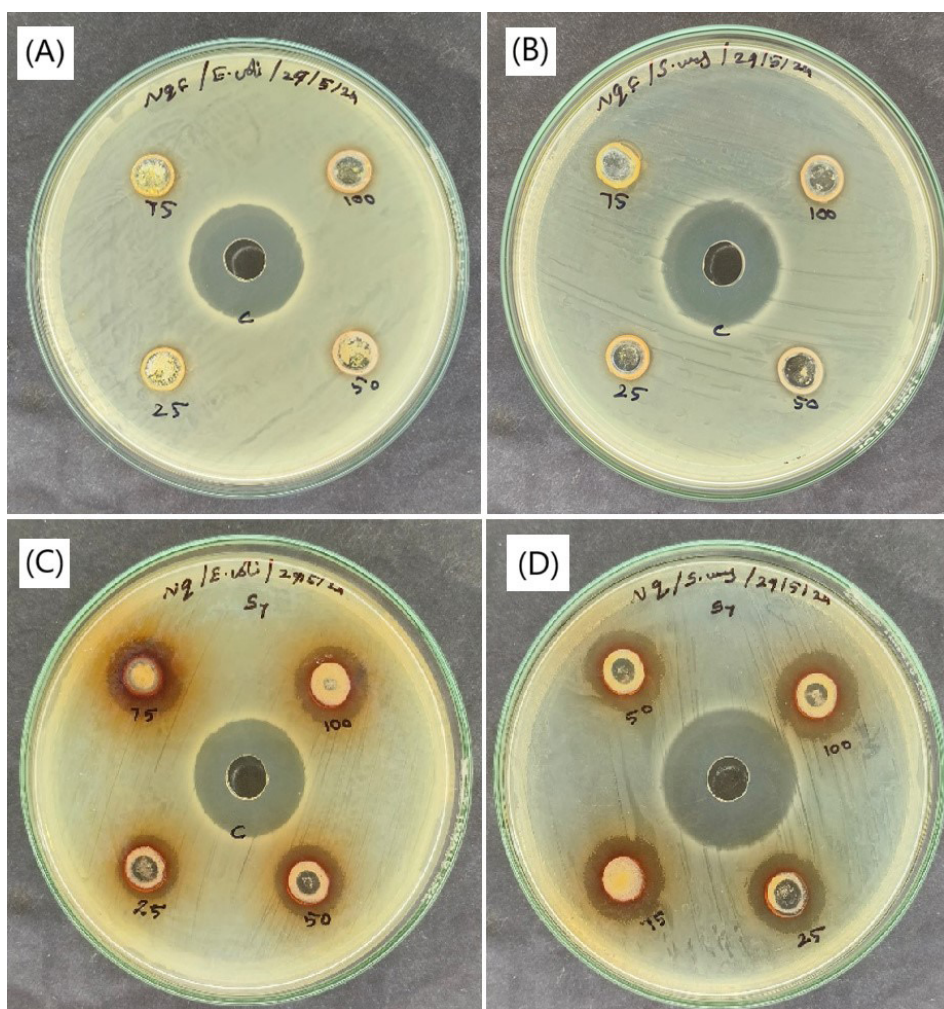


Figure 7: Antimicrobial studies showing (A) pure PNQ with *E. coli*, (B) pure PNQ with *S. aureus*, (C) PNQ nanodispersion (S6) with *E. coli*, and (D) PNQ nanodispersion (S6) with *S. aureus*.

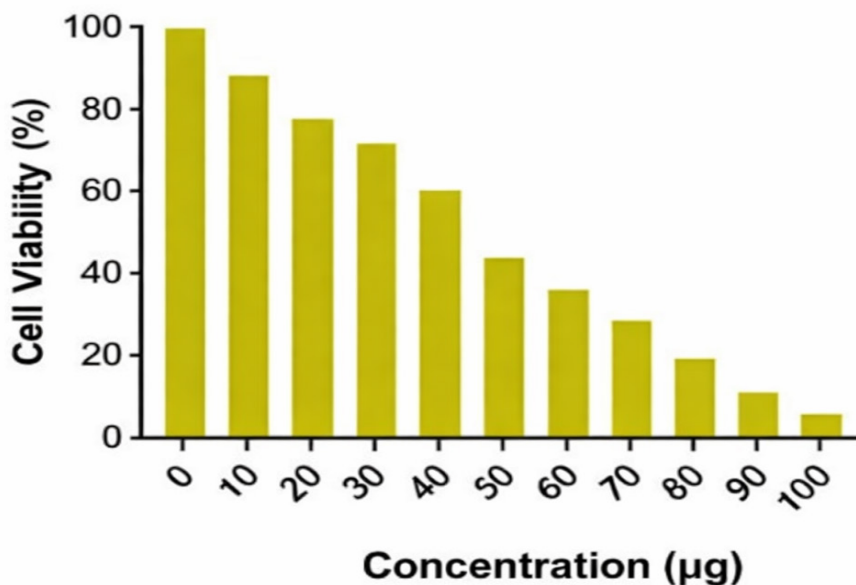


Figure 8: MTT absorption values for PNQ nanodispersion (S6).

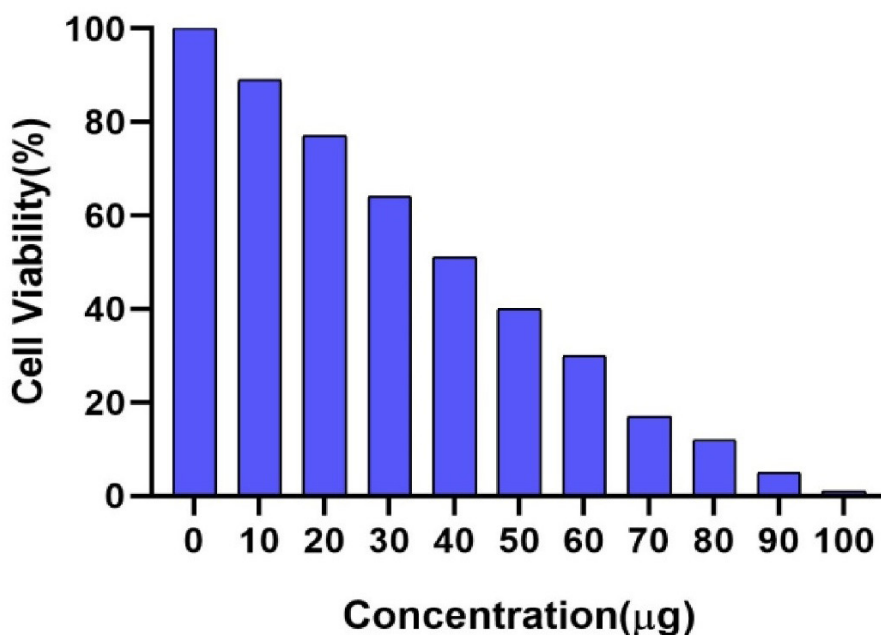


Figure 9: MTT absorption values for PNQ Pure drug.

Cytotoxicity analysis (MTT assay)

The inhibitory concentration (IC_{50}) is the amount of drug needed to inhibit half of the cells' biological activity. Figure 8 summarizes the MTT absorption values for the PNQ formulation. In the PNQ pure drug, the viability of the cell count decreased as the concentration of the drug increased. Figure 9 shows the changes in viability of Hep-g2 cells after treatment with a control and three treatments. The figures clearly demonstrated a substantial decrease in cell count in the treated Hep-g2 cells with formulation S6 compared to the control.

The IC_{50} for the pure PNQ drug was found to be 38.22 ± 0.05 µg/mL. In the PNQ formulation, the cell count viability decreased as the drug concentration increased, with an IC_{50} value of 46.35 ± 0.05 µg. Although the inherent activity of a pure drug might have been higher, the formulations contained inactive ingredients that did not enhance the drug's effect and sometimes slightly impeded the body's ability to absorb the pure drug. However, formulations are a crucial part of safe and effective drug delivery.

CONCLUSION

Casein micelles primarily stabilized the PNQ. The high-pressure homogenizer helped reduce the particle size to nanosize by optimizing the homogenization time and speed. The average nanodispersion size ranges from 230 nm to 350 nm using the Zeta sizer. The average DLS potential of nanodispersion was -17.6 mV to -17.2 mV. This demonstrates that the dispersion was stable because of the hydrophobicity of the casein-induced micelle formation. FTIR analysis has confirmed the presence of casein-micelle-stabilized PNQ particles. The drug content released in formulation S6 was higher when compared to other formulations. The *in vitro* drug release of the formulation was studied using a dialysis membrane with a pore size of 1000 nm. The formulation released the entire drug in an average time of 30 min. *In vitro* characterizations of the formulation were also carried out, including the DLS, and XRD-SEM. The S6 formulation was made better by taking into account its zeta size of 229 nm, its high stable zeta potential of -17.6 to -17.2 mV, and its faster drug release rate within 15 min, with a high drug content of 89.76±3.7%. The IC₅₀ value for the drug nanodispersion that was made was found to be 46.35±0.05 µg in the cytotoxicity assay MTT. The prepared formulation (S6) has the potential to treat bacterial infections and cancer by improving bioavailability, and it is proposed that future *in vivo* studies be performed to assess the safety and efficacy of the PNQ nanodispersions.

ACKNOWLEDGEMENT

The authors would like to extend their gratitude to Kumaraguru College of Technology, Coimbatore and UCE BIT Campus Anna University, Tiruchirapalli 620024, India for their invaluable technical assistance.

CONFLICT OF INTEREST

The authors declare that there is no conflict of interest.

ABBREVIATIONS

PNQ: Para-naphthoquinone; ENPs: Engineered nanoparticle; ELS: Electrophoretic light scattering; XRD: X-ray diffraction; FBS: Fetal bovine serum.

SUMMARY

This study investigates the development and evaluation of p-naphthoquinone (PNQ) casein nanodispersions for their antibacterial and anticancer properties. The optimized formulation (S6) exhibited a particle size of 229 nm, a zeta potential of -17.6 mV, and a drug content of 89.76%. Characterization techniques confirmed successful encapsulation and a semi-crystalline structure. Rapid drug release was observed, with 75.13% released in 15 minutes. Antibacterial assays demonstrated activity against *E. coli* and *S. aureus*, while cytotoxicity studies revealed promising

anticancer potential with an IC₅₀ value of 46.35 µg. The findings highlight the potential of PNQ nanodispersions to enhance bioavailability and therapeutic efficacy for treating bacterial infections and cancer.

REFERENCES

- Elzoghby AO, Abo El-Fotoh WS, Elgindy NA. Casein-based formulations as promising controlled release drug delivery systems. *J Control Release*. 2011; 153(3): 206-16.
- Mahajan P, Dhoke SK, Khanna AS. Effect of nano-ZnO particle suspension on growth of mung (*Vigna radiata*) and gram (*Cicer arietinum*) seedlings using plant agar method. *J Nanotechnol*. 2011; 2011(1): 696535.
- Haley B, Frenkel E. Nanoparticles for drug delivery in cancer treatment. In *Urologic Oncology: Seminars and original investigations*. 2008; 26(1): 57-64.
- Zhou W, Zhang Y, Li R, Peng S, Ruan R, Li J, *et al.* Fabrication of caseinate stabilized thymol nanosuspensions via the pH-driven method: Enhancement in water solubility of thymol. *Foods*. 2021; 10(5): 1074.
- Santoso B, Repi VV, Umar H. *Nano Technology: Economic Aspects, Applications and Risks*. Ilmu dan Budaya. 2020; 41(71).
- Akbarzadeh A, Samiei M, Davaran S. Magnetic nanoparticles: preparation, physical properties, and applications in biomedicine. *Nanoscale Res Lett*. 2012; 7(1): 1-13.
- Kumar S, Dilbaghi N, Saharan R, Bhanjana G. Nanotechnology as emerging tool for enhancing solubility of poorly water-soluble drugs. *Bionanoscience*. 2012; 2(4): 227-50.
- Navarro-Tovar G, Vega-Rodríguez S, Leyva E, Loredó-Carrillo S, de Loera D, López-López LI. The relevance and insights on 1,4-naphthoquinones as antimicrobial and antitumoral molecules: A systematic review. *Pharmaceuticals*. 2023; 16(4): 496.
- Bouhadir K, Atallah H, Mezher R, Fatfat M, Gali-Muhtasib H, Elaridi J. Synthesis and biological assessment of novel acylhydrazone derivatives of 2-methyl-1, 4-naphthoquinone. *Org. Commun*. 2017; 10(4): 259-72.
- Kojima H, Sakurai K, Kikuchi K, Kawahara S, Kirino Y, Nagoshi H, *et al.* Development of a fluorescent indicator for nitric oxide based on the fluorescein chromophore. *Chem Pharm Bull (Tokyo)*. 1998; 46(2): 373-5.
- S. Shukla, R. S. Srivastava, S. K. Shrivastava, A. Sodhi and P. Kumar. Synthesis, Molecular Docking and Biological Evaluation of 4-Cycloalkylideneamino 1, 2-Naphthoquinone Semicarbazones as Anticancer agents. *Asian Pacific Journal of Tropical Biomedicine*. 2012; 2(2): S1040-6.
- Prachayasittikul V, Pingaew R, Worachartcheewan A, Nantasenamat C, Prachayasittikul S, Ruchirawat S, Prachayasittikul V. Synthesis, anticancer activity and QSAR study of 1, 4-naphthoquinone derivatives. *European Journal of Medicinal Chemistry*. 2014; 84: 247-63.
- Bhasin D, Chettiar SN, Etter JP, Mok M, Li PK. Anticancer activity and SAR studies of substituted 1,4-naphthoquinones. *Bioorg Med Chem*. 2013; 21(15): 4662-9. doi: 10.1016/j.bmc.2013.05.017. Epub 2013 May 18.
- Freidus LG, Kumar P, Marimuthu T, Pradeep P, Choonara YE. Theranostic mesoporous silica nanoparticles loaded with a curcumin-naphthoquinone conjugate for potential cancer intervention. *Frontiers in Molecular Biosciences*. 2021; 8: 670792. -
- Chakraborty A, Dhar P. A review on potential of proteins as an excipient for developing a nano-carrier delivery system. *Critical Reviews™ in Therapeutic Drug Carrier Systems*. 2017; 34(5).
- De Kruif CG, Holt C. Casein Micelle Structure, Functions and Interactions. In: *Advanced Dairy Chemistry—1 Proteins*. Springer US; 2003. p. 233-76.
- Zahariev N, Marudova M, Milenkova S, Uzunova Y, Piliicheva B. Casein micelles as nanocarriers for benzydamine delivery. *Polymers (Basel)*. 2021; 13(24): 4357.
- Głab TK, Boratyński J. Potential of casein as a carrier for biologically active agents. *Top Curr Chem (J)*. 2017; 375(4): 1-20.
- O'Kennedy BT. Caseins. In: *Handbook of Food Proteins*. Elsevier; 2011. p. 13-29.
- Dahmash EZ, Ali DK, Alyami HS, AbdulKarim H, Alyami MH, Aodah AH. Novel thymoquinone nanoparticles using poly(ester amide) based on L-arginine-targeting pulmonary drug delivery. *Polymers (Basel)*. 2022; 14(6): 1082.
- Chu B-S, Ichikawa S, Kanafusa S, Nakajima M. Preparation and characterization of β-carotene nanodispersions prepared by solvent displacement technique. *J Agric Food Chem*. 2007; 55(16): 6754-60.
- Gupta V, Trivedi P. *In vitro* and *in vivo* characterization of pharmaceutical topical nanocarriers containing anticancer drugs for skin cancer treatment. *Lipid Nanocarriers for Drug Targeting*. 2018; 563-627.
- Vladár AE, Hodoroaba VD. Characterization of nanoparticles by scanning electron microscopy. In *Characterization of nanoparticles 2020* (pp. 7-27). Elsevier.
- Petit S, Madejova J. Fourier transform infrared spectroscopy. In *Developments in clay science 2013 Jan 1* (Vol. 5, pp. 213-31). Elsevier.
- Raval N, Maheshwari R, Kalyane D, Youngren-Ortiz SR, Chougule MB, Tekade RK. *Basic Fundamentals of Drug Delivery*. Academic press. 2019; 369-400.
- D'Souza S. A review of *in vitro* drug release test methods for nano-sized dosage forms. *Adv Pharm*. 2014; 2014: 1-12.

27. Dang Y, Guan J. Nanoparticle-based drug delivery systems for cancer therapy. *Smart Mater Med.* 2020; 1: 10-9.
28. Gonalimali FD, Lin J, Miao W, Xuan J, Charles F, Chen M, Hatab SR. Antimicrobial properties and mechanism of action of some plant extracts against food pathogens and spoilage microorganisms. *Frontiers in microbiology.* 2018; 9: 1639.
29. Balouiri M, Sadiki M, Ibensouda SK. Methods for *in vitro* evaluating antimicrobial activity: A review. *J Pharm Anal.* 2016; 6(2): 71-9.
30. Chang HP, Cheung YK, Shah DK. Discovery and development of ADCs: obstacles and opportunities. *Overcoming Obstacles in Drug Discovery and Development.* 2023; 75-106.
31. Sigmaaldrich.com. [cited 2024 Aug 9]. Available from: <https://www.sigmaaldrich.com/IN/en/technical-documents/technical-article/cell-culture-and-cell-culture-analysis/imaging-analysis-and-live-cell-imaging/cell-viability-and-proliferation>
32. Denizot F, Lang R. Rapid colorimetric assay for cell growth and survival. *J Immunol Methods.* 1986; 89(2): 271-7.
33. Swinney DC. Molecular mechanism of action (MMoA) in drug discovery. In *Annual Reports in Medicinal Chemistry* 2011; 46: 301-17. Academic Press.
34. Agarwala N, Rohani L, Hastings G. Experimental and calculated infrared spectra of disubstituted naphthoquinones. *Spectrochim Acta A Mol Biomol Spectrosc.* 2022; 268(120674): 120674.
35. Sahoo SK. Formulation development and bioavailability assessment of aripiprazole by self-nanoemulsifying drug delivery systems. *Asian Journal of Pharmaceutics (AJP).* 2018; 12(03).
36. Yang L, Qin X, Kan J, Liu X, Zhong J. Improving the physical and oxidative stability of emulsions using mixed emulsifiers: Casein-octenyl succinic anhydride modified starch combinations. *Nanomaterials (Basel).* 2019; 9(7): 1018.
37. Yao Y, Zhou Y, Liu L, Xu Y, Chen Q, Wang Y, *et al.* Nanoparticle-based drug delivery in cancer therapy and its role in overcoming drug resistance. *Front Mol Biosci.* 2020; 7: 193.
38. Gutierrez SMV, Hazell KK, Simonsen J, Robinson SC. Description of a Naphthoquinonic Crystal Produced by the Fungus *Scytalidium cuboideum*. *Molecules.* 2018; 23(8): 1905.

Cite this article: Duraikannu AM, Muthusamy S, Rajesh TP. Formulation and Evaluation of P-Naphthoquinone Casein Nanodispersions and their Antibacterial and Anticancer Activities. *Indian J of Pharmaceutical Education and Research.* 2026;60(2):717-28.